Construction of the Facility for Aluminium Alloys Electromagnetic Stirring During Casting

Piotr Mikolajczak[1(✉)], Jerzy Janiszewski[2], and Jacek Jackowski[1]

[1] Institute of Materials Technology, Politechnika Poznańska, Poznań, Poland
Piotr.Mikolajczak@put.poznan.pl
[2] Institute of Electrical Power Engineering, Politechnika Poznańska, Poznań, Poland

Abstract. The reuse of aluminium, recycling, leads to an increase in the content of alloying elements, including iron. The Fe-rich intermetallic phases called platelets or needles β-Al_5FeSi are hard, brittle and have a highly detrimental effect on the properties of alloys and castings. The construction of facility was proposed, built and its parameters were described. The facility construction allows the castings to be solidified in moulds with a diameter up to 70 mm under intensive stirring in sample castings to decrease negative effect of Fe-rich phases. Facility included the set of coils for rotating magnetic field generation, autotransformers, thermal conditions control unit, thermal insulations, cooler for coils protection, teslameter and brass water-cooled chiller. The construction allowed for bulk solidification with equiaxed dendritic structure in the whole sample. The subject of the presence of forced convection to improve casting properties in the bulk solidification and in the directional solidification was discussed.

Keywords: Casting · Electromagnetic stirring · Aluminium alloys · Intermetallic phases · β-Al_5FeSi precipitate

1 Introduction

Cast aluminium alloys enriched with silicon, silumins have been categorised as hypoeutectic, eutectic and hypereutectic. The characteristic features in hypoeutectic silumins include α–Al dendritic precipitates, while in the case of the hypereutectic ones, silicon precipitates. The structure of hypoeutectic silumins consists of α–Al dendrites and the aluminium-silicon eutectics located between dendrites and is determined by the chemical composition, melting, solidification conditions and thermal treatment. The structure of silumins is characterised by a number of parameters such as grain size, primary and secondary dendrite arm spacing, size and location of secondary phase precipitations as well as macro- and micro-porosities. Popular cast alloys are e.g. AK7, containing 7% of silicon, and also AK9, AK12.

Alloys can be produced from technical aluminium and alloying additions, but it is economically more advantageous to apply aluminium scrap recycling. At the stage of use of products (e.g. machinery, vehicles) and at the stage of scrap selection, parts

B. Gapiński et al. (Eds.): *Advances in Manufacturing II* - Volume 4, LNME, pp. 164–175, 2019.
https://doi.org/10.1007/978-3-030-16943-5_15

made of aluminium alloys co-exist with cast-steel, cast-iron and other products. The important role in the casting practice is also played by the use of steel tools during the melting and casting processes. At the stage of processing of the aluminium scrap only, the recycling covers cast alloys and alloys for plastic forming, that is, those which are different in terms of their chemical composition. The multiple recycling of silumins may result in accumulating and increasing the content of iron in the alloys. The reuse of aluminium, recycling, leads to an increase in the content of alloying elements, especially iron.

The structure of hypoeutectic silumins consists of α–Al phase dendrites and aluminium-silicon eutectics. As well as aluminium and silicon, silumins contain small amounts of magnesium, copper, iron, manganese, nickel, zinc and other elements, and their presence complicates the microstructure and the process of its formation. In multi-element alloys, the process of formation of the structure gets complicated and leads to various precipitates. Then, as well as dendrites and eutectic, smaller amounts of precipitation are visible on the microstructures. These microstructures include alloying additions, e.g. intermetallic phases which contain metallic and non-metallic elements.

1.1 Fe-Rich Intermetallic Phases in AlSi Alloys

The formation of Fe-rich intermetallic phases [1–3] is caused by very low solubility of this element in α–Al (max. 0.05%). These precipitates are characterised by the structure, shape and chemical composition, conditions of nucleation, crystallisation and growth. The respective phases may be formed in the eutectic or peritectic reaction, and the precipitations may take the form of needles, platelets, blocks or Chinese script, or their shape may be angular or dendritic. They may be present in the inter-dendritic area or inside the α–Al dendrites. The earliest microscopic examinations reported a wide variety of AlFeSi precipitates, which were classified on the basis of morphology into three groups: polyhedral crystals, Chinese script and thin platelets or needles. Most of these equilibrium phases occurring at low cooling speed in low-alloyed AlSi were characterised [1–4] as θ-Al_3Fe, α-Al_8Fe_2Si, β-Al_5FeSi, α-$Al_{12}Fe_3Si_2$, δ-Al_4Si_2Fe [5, 6], additionally, metastable phases as Al_6Fe and α-$Al_{20}Fe_5Si_2$. The analysed chemical compositions of precipitates may differ in terms of the specified phase, e.g. for Al_6Fe, the content of elements was measured in the range of 73.16–73.44% Al, 1.49–1.76% Si, 25.92–27.04% Fe with stoichiometry $Al_{6.05}FeSi_{0.114}$, while for α-AlFeSi in the range of 59.46–74.48% Al, 6.87–9.34% Si, 23.88–30.75% Fe with stoichiometry $Al_{9.1}Fe_2Si_{0.87}$, and for β-AlFeSi in the range of 55.27–63.52% Al, 13.06–15.25% Si, 26.41–26.99% Fe with stoichiometry $Al_{4.20}FeSi_{1.13}$ [4]. In AlSi alloys, the most frequent intermetallic iron precipitates are the following phases: β-Al_5FeSi (also marked as β, β-AlFeSi) and α-Al_8Fe_2Si (α, α-AlFeSi).

In AlSi alloy castings, there are β-Al_5FeSi phases (Fig. 1), called as platelets or needles, which are hard, brittle and which have a highly detrimental effect on the properties of alloys and castings. The size of β-Al_5FeSi may range between 40 and 150 μm [1], 5 and 10 μm [2] or it may be much bigger. The marking "β-Al_5FeSi", which interchangeable with $Al_9Fe_2Si_2$, follows from the stoichiometry [4] in the range from $Al_{4.20}FeSi_{1.13}$ to $Al_{4.98}FeSi_{1.09}$. The β-Al_5FeSi intermetallic phases are of great

significance to the properties of AlSi alloys and the produced castings as they affect a number of their technological and performance properties:

- Porosity and feedability – the occurrence of intermetallic phases, and especially β causes an increase in porosity in castings [7], as they block the feeding flow of liquid alloy in castings by affecting the nucleation of pores and lowering the interdendritic permeability [8],
- Cracks and fatigue crack – β phases are crack initiation sites [9], an increase in the content of Fe reduces the fatigue strength for long load periods (>10^6 cycles) [10], furthermore as large and elongated β-Al_5FeSi whose longer dimension is perpendicularly oriented towards the set load are subject to decohesion [11], while the parallel-oriented phases are subject to longitudinal cracking and fragmentation,
- Hardness – the presence of intermetallic phases causes an increase in hardness from 75 to 90 HB [12] at an increase in iron from 0.1% (and the corresponding fraction of the area in the microstructure occupied by β-Al_5FeSi SF = 0.2%) to 0.9% Fe (SF = 3.8%),
- Strength – as the length of average β increases (from 50 to 250 μm), a decrease is observed with regards to elongation (from 6 to 0.5%) and tensile strength (from 260 to 170 MPa) in the industrial aluminium alloy 319.2 [13]. It has been observed that an addition of 0.20% Fe (which causes the presence of β-Al_5FeSi) to the industrial A356 alloy increases the yield strength from 172 to 193 MPa, but decreases the tensile strength from 269 to 260 MPa [14]; an increase in the content of iron from 0.11 to 0.6% reduces the impact strength from 4 to 2 J [15, 16],
- Formability – the iron content and the presence of β compromises the formability of castings [17],
- Adhesion – intermetallic phases containing iron and manganese trigger a positive effect in the high-pressure casting technology, as they reduce the adhesion of castings in permanent moulds [18], facilitate their removal from the mould and improve the quality of casting surface,
- Corrosion – the presence of precipitates which contain iron and manganese causes corrosion (dissolution) of the aluminium matrix directly around such precipitates in Al alloy castings [19].

To sum up, β-Al_5FeSi phases are nuclei of pores and cause an increase in porosity in castings and reduce the feedability by the reduction in the interdendritic flow. They constitute crack initiation sites, owing to which they reduce fatigue strength and immediate strength as well as impact strength and elongation. Furthermore they reduce formability. The positive effect of the presence of iron in silumins and its addition is the reduction in the adhesion of castings in permanent moulds, in die casting and pressure casting.

In order to avoid the harmful effect a number of methods was developed to avoid the harmful effect of intermetallic precipitates. Iron can be removed by electrolysis, which is very expensive. The supplementation of silumins by manganese, lithium, potassium, strontium, calcium does not guarantee efficiency, and the excess of e.g. manganese compromises the mechanical properties. These additions do not guarantee efficiency. They require control of the chemical composition; the interactions between the respective additions may negatively affect the alloy properties. Heat treatment

causes the separation of phases, but does not remove porosity. Melt superheating requires energy, intensifies the furnace wear as well as gas pick-up and formation of oxides. The solidification conditions are limited by the type of mould, the metal one and not the sand one. Precipitation and sedimentation require longer time to carry out the treatment, and centrifugal separation is technically possible only for small ingots.

Almost all studies regarding Fe-rich intermetallic phases were aimed at the evaluation of its harmful effect on the properties of alloys or improvement of the situation by the application of the above-mentioned methods. There are only a few publications regarding the influence of forced flow by way of electromagnetic or mechanical stirring.

In the studies of the team of professor Fang [20], during the intensive mechanical dispersion stirring of the semi-liquid melt using rheo-diecasting, the transformation of β needles to blocks was demonstrated. It was observed that iron phases for the LM25 alloy (AlSi7Mg0.2–0.6Fe0.5) had been shortened and in the case of the LM24 alloy (AlSi8Cu3Fe1.3), β-Al_5FeSi were completely eliminated. Professor Ghomashchi's team [21], as a result of electromagnetic stirring during the solidification of the cylindrical specimen made of the AlSi6.8Fe0.8 alloy with a diameter of 76 mm and length of 300 mm, demonstrated the shortening of intermetallic phases in the specimen cast in the sand form and in the copper casting die. However the paper does not include data regarding the electromagnetic field density and the exact sampling site. While testing the AlSi7Fe1 alloy, Steinbach and Ratke [22, 23] observed an increase in the length of β-Al_5FeSi needles under the influence of forced flow. The mentioned publications do not contain the data regarding, e.g. the sampling site, the convection conditions for stirring and the modification mechanism, therefore the state of knowledge about the influence of convection on the intermetallic phases required additional research.

In the current paper, it was presented a device designed for introducing forced convection during the production of sample castings and the literature data on the influence of stirring on the microstructure and Fe-rich intermetallic phases in the bulk solidification and in the directional solidification were discussed.

2 Methodology

The designed device was intended to conduct solidification in the rotating magnetic field RMF. It was assumed to construct a device for sample castings using electromagnetic fields in accordance with a number of guidelines below.

The device should allow solidification in the broad possible range of thermal conditions, temperature gradient and cooling rate. In the first design variant, the solidification of the cylindrical samples was planned, the lower part of which contacts the water cooled chiller introducing a large temperature gradient and directed solidification (not directional solidification) from bottom to top. In addition to the cooler, the directed solidification should be caused by a mold made of a material with low thermal conductivity or mould possibly heated (600–1000 °C) to slow cooling down the lateral surface of the sample and supporting directed solidification starting from the surface of brass water-cooled chiller. In the second design variant, it should be possible to cool

evenly and solidify at a low temperature gradient and low cooling rate, maintaining the bulk solidification in the whole sample casting. The cylindrical sample should solidify without contact with the cooler, in a form made of material with low thermal conductivity or capable of being heated to high temperatures (600–1000 °C) for slow cooling, low temperature gradient and long-lasting electromagnetic field introducing stirring in the studied alloys, melt or forming mushy.

The device should be able to measure the thermal conditions in the casting and mould, water cooling of the cooler, thermal protection of the coils and measurement of the electromagnetic field. The electromagnetic field should be generated with electromagnetic coils located around the sample.

3 Results

The designed and built facility for solidification in the magnetic field allows the castings to be solidified in moulds with a diameter up to 70 mm (Figs. 1 and 2). In this device, the magnetic field is generated owing to the set of coils (Fig. 1b) powered from the network in the one-phase system, via an autotransformer, or in the three-phase system via toroidal transformers. The Tufvassons autotransformer (Sigtuna, Sweden), type KIEA 4, with the input voltage of 230 V (50–60 Hz) and output voltage ranging between 0 and 260 V (3.8 A), as well as Miflex MKSP 5P capacitors (60 μF, 450 V/500 V) and Breve TTS 150/Z toroidal transformers (primary voltage: 230 V 50/60 Hz and secondary voltage 12 V 6.0 A) were used.

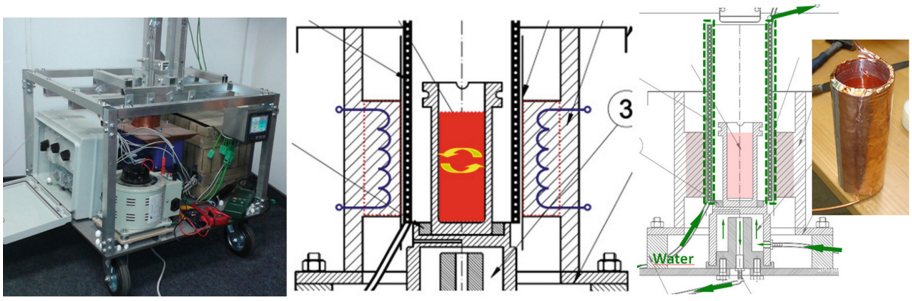

Fig. 1. Diagram of the device intended for solidification in the magnetic field: (a) photo with the visible temperature recorder, autotransformer for one-phase power supply and set of switches for three-phase power supply by means of toroidal transformers, (b) diagram of the location of a specimen in the graphite crucible and the field-generating coils, (c) diagram of the location of the copper chiller that separates coils from the crucible with liquid melt.

In order to control thermal conditions, we made sure that the temperature could be measured in the solidifying casting, mould and chiller and in the winding of coils heated during power supply. There were applied thermocouples, type K (TP-203) and

the APAR AR 207 data recorder (Fig. 1a). In order to protect the winding of the coils against heating radiating from the casting and the crucible, we built a cooler (Fig. 1c) in the form of a spiral made of a copper tube, supplied with district cooling water (water output 5–10 L/min.). Furthermore, in order to protect the coils, and mainly to slow down the cooling and solidification of specimens, thermal insulation was installed around the entire crucible (Fig. 2b and c). We used the Fiberfrax Sibral insulation (Unifrax, Tonawanda, USA) with conductivity of 0.1 W/mK and the Porogel Optima Evergel aerogel insulation mat (Aerogels Nanotechnology, USA) with conductivity of 0.02 W/mK. The application of the insulation ensured conditions for bulk solidification at low cooling rate (0.112 K/s within the liquidus-solidus temperature range) and low temperature gradient (0.143 K/mm). We installed the magnetic field distribution meter, the Extech MF 100 teslameter (Extech, Fig. 2a) with the transverse probe in the device, or optionally used the TH26 gaussmeter (Aspan, Warsaw). At different power supply values, there were measured the field density and achieved the value of 11 mT (at the power supply value 45 V and 10 A), and the estimated rotating speed of the stirred liquid melt was 2.1 rev./s.

In order to ensure the bulk solidification we applied the thermal insulation around the entire specimen, but optionally the directed solidification (not directional solidification) from the lower brass water-cooled chiller was also possible. In such a configuration, the mould comprises tubes with a diameter up to 38 mm and approximate length of 300 mm, made of graphite or moulding compound.

The designed and built facility for solidification in the magnetic field allowed for bulk solidification. In order to ensure the structure with the equiaxed dendrites, the melt was subjected to slow cooling. A cylindrical specimen, with a diameter of 38 mm and

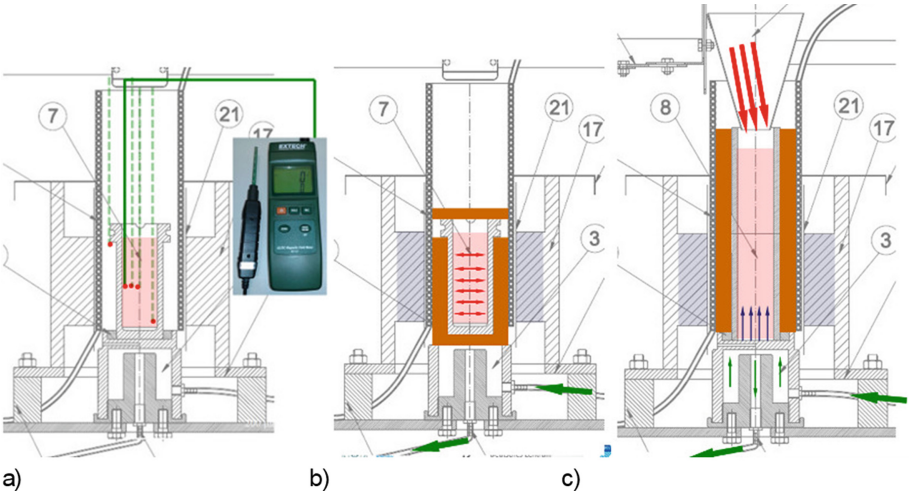

Fig. 2. Diagram of the device intended for solidification in the magnetic field: (a) diagram of the location of a teslameter with probe locations, (b) diagram of the location of a thermal insulation around the whole graphite crucible, for bulk solidification conduction, (c) diagram of the location of the mould, thermal insulation (on the lateral surface of the mould) and the brass water-cooled chiller on bottom side.

length of 55 mm was melted and superheated up to the temperature of 810 °C in a graphite crucible, then transferred to the built solidification facility and cooled down in the same thermally insulated crucible. The temperature measurement in the alloy sample and in the graphite crucible indicated the cooling rate within the liquidus-solidus range - 0.112 K/s and temperature gradient - 0.143 K/mm. The joint heating and cooling of the specimen and the crucible ensured slow cooling and solidification within the entire space of the studied alloy. The low temperature gradient and low cooling rate resulted in the formation of the equiaxed structure in the entire sample. The solidification was conducted without or with the stirring generated by the rotating magnetic field with a stream density of 11 mT.

4 Discussion

In castings, columnar dendrites characteristic for the directional solidification occur only in the surface layer, while inside castings, the solidification is close to the bulk solidification and there occurs equiaxed dendritic structures, therefore, the analysis of fluid flow effect on the microstructure should include both, directional solidification and bulk solidification conditions.

In the paper [24] the forced convection was studied in terms of the impact on the equiaxed dendritic structure (in bulk solidification) of AlMgSi alloys with Fe-rich and Mn-rich intermetallics. The average length of β-Al_5FeSi intermetallic phases decreased by 20% in the AlSi5Fe1.0 alloy, while in the AlMg5Si5Fe1.0 alloy by 5%, and in AlMg5Si5Fe1.0Mn1.0, there were no changes. The number density of β increased in all alloys. The Mn-rich intermetallic phases decreased their size by 9% and the number density increased, while the spacing between the aluminium-silicon eutectic and magnesium-silicon platelets did not indicate an unambiguous change under the influence of convection. Based on the Calphad calculations, it is known that in the AlSi5Fe1.0 alloy, the β-Al_5FeSi phase is the second one to start to grow at the temperature of 608 °C after α-Al rosettes, which precipitated in 40%, without blocking the convection and the shortening of β platelets by 20%. On the other hand, in the AlMg5Si5Fe1.0 alloy β precipitate from the temperature of 592 °C, and magnesium-silicon eutectic from 581 °C, and there are no changes in the dendrite arm spacing, and Fe phases were shortened by 5% and not 20%.

It was proven that the presence of Mg_2Si eutectic weakens the effects of forced convection at the final solidification stage and as a consequence of this, the change in the dendrite arm spacing as well as the shortening of β-Al_5FeSi phases. It does not block, however, the growth of the α-Al phase in the form of rosettes instead of equiaxed dendrites occurred.

Experiments [24] showed the advantageous effect of forced convection in the bulk solidification on the shortening of β-Al_5FeSi phases and a reduction in the secondary dendrite arm spacing, however, they indicated the significance of occurrence of precipitates (e.g. Mg_2Si), which could block the flows and changes in the microstructure.

In publications [22–24], there was proven that forced convection reduces the primary dendrite arm spacing (PDAS) but does not affect the secondary dendrite arm spacing (SDAS), specific surface (Sv) of dendrites and spacing of the aluminium-

silicon eutectic (Al-Si). This is possible because the values of PDAS depend on the solute supercooling which reaches even several hundred micrometres into the depth of the mushy zone, while SDAS depends on the coarsening process which takes place much deeper in the mushy zone. Because of the absence of Fe-rich intermetallic phases, the convection only reaches the upper parts in the mushy zone (Fig. 2c), but not other, central and lower regions, located deeply at the base of columnar dendrites.

In paper [25], was demonstrated the possibility of shortening of β-Al_5FeSi phase precipitates by 24% as well as an increase in their number density by the introduction of the forced convection, and the lack of influence of the melt stirring on the Fe-rich intermetallic phases, blocky shaped, Chinese script, very thick and curved phases.

Under the directional solidification conditions [25] was performed a detailed analysis of the length of β-Al_5FeSi phases and pointed to the 20% shortening of needles in the dendritic area and 9% elongation in the eutectic zone, and a clear increase in the number density under the influence of forced convection, stronger in the eutectic centre (42%) than in the dendritic outer ring of specimens (17%). Based on histograms, it was demonstrated that the forced convection caused an increase in the number density of short β-Al_5FeSi with lengths ranging between 0 and 40 μm, leading to a smaller average length of β needles, i.e. the presence of long β was compensated by the greater number of short phases. The studies demonstrated that the application of forced convection is more efficient in the shortening of β-Al_5FeSi phases than a reduction in the content of iron from 1% Fe to 0.2% Fe, and the flow with a rate of about 10.5 mm/s in the dendritic structure enables the reduction in their size by 24%, i.e. the application of such stirring in the castings may shorten the needles and reduce their negative impact on the casting properties. The results did not show any relationship between stirring and the occurrence of other Fe intermetallic phases, including blocky shaped phases (α-Al_8Fe_2Si) and Chinese script. It was also pointed to the variation of spatial conditions for nucleation and growth of β-Al_5FeSi.

In directional solidification conditions by temperature gradient 3 K/mm, the magnetic field with a density of 6 mT triggers the azimuthal flow [26] with a velocity of 10 mm/s, as well as the axial and radial flows which transport the colder liquid melt and solute from the dendrite tip towards the centre and then towards the higher temperatures, reaching the area 12 mm above the dendrites, with the temperature higher by 36 °C. β-Al_5FeSi intermetallics which start to grow several millimetres after the dendrite tips, and which are transported to the region characterised by higher temperatures, are subject to melting and dissolution, and such a fragmentation and melting acts as the source of nuclei of new precipitates, causing a higher number density of short phases and finally, a reduction in the average length of β-Al_5FeSi platelets.

In the paper [26] the X-ray tomography revealed β phases which appeared to be curved, bent, branched, with twining, crossing, hole-shaped, wavy-shaped and formed on and around porosities, as well as extra-large platelets. The analysis of convective movements indicated the mechanism of shortening of the β-Al_5FeSi phases. The growth of large and complex phases may lead to a reduction in the liquid melt flow between dendrites and to a decrease in the permeability of the mushy zone, complex microstructures in castings and variable alloy properties. It may also require modifications in the technological process. The advantage of the publication, except the presentation of different β phase morphologies, and in relation to other tomographic

investigations [27–29], is the investigation of specimens formed in the controlled thermal and convective conditions without destruction (metallographic etching) of the dendritic and eutectic regions.

The equilibrium phase diagrams, solidification paths, mass fractions of phases were calculated and the forecasts for the solidification front (mushy zone) shape under forced convection conditions in AlSiFe alloys were developed [30]. The methodology for use of diagrams of the mass fraction of precipitated phases, which was developed on the basis of Calphad thermodynamic calculations, allowed the mapping of the solidification front under conditions of directional solidification and forced convection. Analysis of the ternary equilibrium phase diagram (Al-Si-Fe) demonstrated the variation of solidification paths, while diagrams of mass fractions of the phases demonstrated significant changes in the amount of precipitated phases under the influence of stirring. The maps of solidification front (mushy zone) showed the liquid channel, in which the β-Al_5FeSi phase might nucleate and grow intensively before the appearance of α-Al dendrites, and also the reverse situation in the external dendritic part of the samples.

In paper [30], it was proven that the forced convection under directional solidification conditions, caused changes in: the sequence of precipitation and in temperatures characteristic for the formation of phases, as well as in the shape and length of the solidification front. It also affected the place of nucleation and the movement of intermetallic phases in AlSiMn alloys. The studies demonstrated the formation of the solidification front with the dense dendritic structure, central area free of dendrites and $Al_{15}Si_2Mn_4$ phases, where the possibility of flow of intermetallic precipitates is small. Additionally, the formation of the shorter dendritic front with $Al_{15}Si_2Mn_4$ intermetallic phases, which can nucleate, grow and be freely transported in the area above the dendrite tips was also demonstrated.

Developed solidification front forecasts with the distribution of α-Al dendrites as well as β-Al_5FeSi and $Al_{15}Si_2Mn_4$ phases were presented in [30]. The β-Al_5FeSi phases start to grow mainly at temperatures lower than the temperatures of formation of α-Al dendrites; therefore, they are more often than not transported between the dendrites and below the dendritic front tip. $Al_{15}Si_2Mn_4$ nucleate at higher temperatures than β and in many sites before α-Al, therefore, they can grow and be transported above the dendritic zone, forming a significant part of the mushy zone. Such a transport with forced convective movements allows the $Al_{15}Si_2Mn_4$ precipitates to be distributed more evenly on the cross-section of solidified specimens, while β are more concentrated in the central part. It is necessary to emphasise the variable permeability of the dendritic area with β-Al_5FeSi phases and the liquid melt area with the morphologically varied Mn-rich phases which are freely transported within that area. The change in length and shape of the dendritic area, Si content (dendritic structure) and location of the respective α-Al, β-Al_5FeSi and $Al_{15}Si_2Mn_4$ phases may significantly affect the permeability in the central and outer part of the specimens, and thus, the variation of convective movements which penetrate the mushy zone.

In the paper [31], there was proposed the methodology of effective calibration of the device designed for directional solidification. The introduction of coefficient M made it possible to shorten the calibration process, and to conduct the solidification process precisely at the assumed temperature gradient, cooling rate and solidification front velocity. In [31] was considered the phenomenon of formation of a gap between

the specimen and the lower furnace in the device designed for directional solidification – Artemis. It was proven that the formation of the gap between the specimen and the chiller was the most important factor that disturbed the course of the controlled directional solidification process.

5 Conclusions

The designed and built facility for solidification in the magnetic field allowed for bulk solidification. In order to ensure the structure with the equiaxed dendrites, the melt was subjected to slow cooling. The low temperature gradient and low cooling rate resulted in the formation of the equiaxed structure in the entire sample. The solidification was conducted without or with the stirring generated by the rotating magnetic field with a stream density of 11 mT.

The constructed facility and the discussed developments of basic knowledge on solidification [24–26, 30, 31] were concerned the method of reduction in the impact of β-Al_5FeSi intermetallic phases under forced convection generated by a device that induces magnetic field around the metal cast into the casting mould and during the casting solidification.

In the paper were discussed scientific achievements targeted at determining the influence of forced convection on nucleation, growth, morphology, spatial distribution of Fe-rich intermetallic phases in aluminium alloys with silicon, containing iron and/or manganese. The mentioned subjects covered:

- the influence of forced convection on the microstructure of alloys [25], where it was observed that convection in the directional solidification process reduces the primary dendrite arm spacing PDAS, while SDAS and Sv stayed almost unchanged,
- the influence of forced convection on intermetallic phases, their morphology and location [25, 26], where it was proved that the β-Al_5FeSi needles became shorter in the dendritic structure and longer in the eutectic region,
- the evaluation of convection conditions during the solidification process [25, 26], a fragmentation and melting acts as the source of nuclei of new precipitates, causing a higher number density of short phases and finally, a decrease in the average length of β-Al_5FeSi platelets,
- the forecast of the solidification front in the directional solidification process [30], it was developed the methodology of application of Calphad-based thermodynamic calculations to forecast the solidification front,
- analysis of conditions of directional solidification for alloys whose composition is similar to that of hypoeutectic silumins [31],
- experiments for the bulk solidification conditions [24], there was demonstrated that intermetallic phases (the shortening of β-Al_5FeSi) and dendrites (a reduction in the dendrite arm spacing) can be modified also during the bulk solidification process,
- the design and construction of the prototype of a casting device in the magnetic field, developed and presented in current paper and applied in [24], based on the developments described in [24–26, 30, 31] the basics of the technology designed to control intermetallic phases and their morphology and spatial distribution.

The results of the above-mentioned studies are an essential contribution into the existing state of the art regarding the production of castings, the process of AlSi alloy solidification, the conditions for formation of the alloy structure and morphology of Fe-rich and Mn-rich intermetallic phases under the natural convection and forced convection.

Acknowledgments. The research leading to these results has received funding from the People Programme (Marie Curie Actions) of the European Union's 7th Framework Programme (FP7/2007-2013) under Research Executive Agency REA grant No. PCIG13-GA-2013-613906.

References

1. Skjerpe, P.: Metall. Trans. A **18A**, 189 (1987)
2. Rilvin, V.G., Raynor, G.V.: Int. Metall. Rev. **3**, 133–152 (1981)
3. Shabestari, S.G.: Mater. Sci. Eng. **A383**, 289–298 (2004)
4. Khalifa, W., Samuel, F.H., Gruzleski, J.E.: Iron intermetallic phases in Al corner of the Al-Si-Fe system. Metall. Mater. Trans. A **34**, 807–825 (2003)
5. Srivastava, A.K., et al.: Acta Mater. **54**, 1741–1748 (2006)
6. Zhang, L., Gao, J., Damoah, L., Robertson, D.: Removal of iron from aluminium – a review. Miner. Process. Extr. Metall. Rev. **33**, 99–157 (2012)
7. Dinnis, et al.: Iron related porosity in Al-Si-Cu foundry alloys. Mater. Sci. Eng., A **425**, 286–296 (2006)
8. Moustafa, M.A.: Effect of iron content on the formation of β-Al_5SiFe. J. Mater. Process. Tech. **209**, 605–610 (2008)
9. Firouzdor, V.: Effect of microstructural constituents on the thermal fatigue life of A319 Al alloy. Mater. Sci. Eng. **A454–455**, 528–535 (2007)
10. Yi, J.Z., et al.: Effect of Fe-content on fatigue crack initiation and propagation in a cast. Mater. Sci. Eng. **386**, 396–407 (2004)
11. Lassance, D., et al.: Micromechanics of room and high temperature fracture in 6xxx Al alloys. Progress Mater. Sci. **52**, 62–129 (2007)
12. Tash, M., et al.: Effect of metallurgical parameters on the hardness and microstructure. Mater. Sci. Eng. **A4430**, 185–201 (2007)
13. Ma, Z., et al.: A study of tensile properties in AlSiCu and AlSiMg alloys. Mater. Sci. Eng. A **490**, 36–51 (2008)
14. Kim, H.Y., et al.: The influence of Mn and Cr on the tensile properties of A356-0.2Fe alloy. Mater. Lett. **60**, 1880–1883 (2006)
15. Chen, Z.W., et al.: The effect of squeeze casting pressure and iron content on the impact energy. Mater. Sci. Eng. **A221**, 143–453 (1996)
16. Ferrarini, C.F., et al.: Microstructure and mechanical properties of spray deposited hypoeutectic Al–Si alloy. Mater. Sci. Eng. **A375–377**, 577–580 (2004)
17. Tash, M., et al.: Effect of metallurgical parameters on the machinability of heat-treated 356 alloys. Mater. Sci. Eng. **A434**, 207–217 (2006)
18. Shahverdi, H.R., Ghomashchi, R., Shabestari, H., Hedjazi, J.: J. Mater. Proc. Technol. **124**, 345–352 (2002)
19. Wei, R.P., Liao, C.M., Gao, M.: A transmission electron microscopy study of constituent particle-induced corrosion in 7075-T6 and 2024-T3 Aluminum Alloys Metall. Mater. Trans. **29A**, 1153 (1998)

20. Fang, X., Shao, G., Liu, Y.Q., Fan, Z.: Effects of intensive forced melt convection on the mechanical properties of Fe containing Al-Si based alloys. Mater. Sci. Eng., A **445–446**, 65–72 (2007)
21. Nafisi, S., Emad, D., Shehata, T., Ghomashchi, R.: Effects of electromagnetic stirring and superheat on the microstructural characteristics of Al-Si-Fe alloy. Mater. Sci. Eng., A **A432**, 71–83 (2006)
22. Steinbach, S., Ratke, L.: Trans. Indian Met. **60**(2–3), 137–141 (2007)
23. Steinbach, S., Ratke, L.: Metall. Mater. Trans. **38A**, 1388–1394 (2007)
24. Mikołajczak, P.: Microstructural evolution in AlMgSi alloys during solidification under electromagnetic stirring. Metals **7**, 89 (2017)
25. Mikołajczak, P., Ratke, L.: The effect of stirring induced by rotating magnetic field on β-Al5FeSi intermetallic phases during directional solidification in AlSi alloys. Int. J. Cast Met. Res. **26**, 339–353 (2013)
26. Mikołajczak, P., Ratke, L.: Interplay between melt flow and the 3D distribution and morphology of Fe-Rich phases in AlSi alloys. Metall. Mater. Trans. A **46A**(3), 1312–1327 (2015)
27. Terzi, S., Taylor, J.A., Cho, Y.H., Salvo, L., Suery, M., Boller, E., Dahle, A.K.: Acta Mater. **58**, 5370–5380 (2010)
28. Dinnis, C.M., Taylor, J.A., Dahle, A.K.: Scripta Mater. **53**, 955–958 (2005)
29. Timpel, M., Wanderka, N., Murty, B.S., Banhart, J.: Acta Mater. **58**, 6600–6608 (2010)
30. Mikołajczak, P., Genau, A., Janiszewski, J., Ratke, L.: Thermo-calc prediction of mushy zone in AlSiFeMn alloys. Metals **7**, 506 (2017)
31. Mikołajczak, P., Ratke, L.: Directional solidification of AlSi alloys with Fe intermetallic phases. Arch. Foundry Eng. AFE **14**(1), 75–78 (2014)